THE JOURNAL OF BIOLOGICAL CHEMISTRY
Vol. 279, No. 33, Issue of August 13, pp. 34388–34396, 2004
Printed in U.S.A.

Association of Excitatory Amino Acid Transporters, Especially EAAT2, with Cholesterol-rich Lipid Raft Microdomains

IMPORTANCE FOR EXCITATORY AMINO ACID TRANSPORTER LOCALIZATION AND FUNCTION*

Received for publication, April 8, 2004, and in revised form, June 4, 2004
Published, JBC Papers in Press, June 8, 2004, DOI 10.1074/jbc.M403938200

Matthew E. R. Butchbach‡§¶, Guilian Tian‡§, Hong Guo‡, and Chien-liang Glenn Lin‡§‖‡‡**

*From the ‡Department of Neuroscience, the §Ohio State Biochemistry Program, the ‖Neuroscience Graduate Studies Program, and the **Integrated Biomedical Sciences Graduate Program, The Ohio State University, Columbus, Ohio 43210*

In the present study, we investigated the role of membrane cholesterol in the function of glutamate transporters. Depletion of membrane cholesterol by methyl-β-cyclodextrin resulted in reduced Na^+-dependent glutamate uptake in primary cortical cultures. Glial glutamate transporter EAAT2-mediated uptake was more sensitive to this effect. Cell surface biotinylation and immunostaining experiments revealed that the loss of cholesterol significantly altered the trafficking of EAAT2 to the plasma membrane as well as their membrane distribution. These effects were also observed in neuronal glutamate transporter EAAT3 but to a lesser extent. Furthermore, the treatment of mouse brain plasma membrane vesicles with methyl-β-cyclodextrin resulted in a significant reduction in glutamate uptake, suggesting that cholesterol depletion has a direct effect on the function of the glutamate transporters. Plasma membrane cholesterol is localized within discreet microdomains known as lipid rafts. Analyses of purified lipid raft microdomains revealed that a large portion of total EAAT2 and a minor portion of total EAAT1, EAAT3, and EAAT4 were associated with lipid rafts. Artificial aggregation of lipid rafts *in vivo* resulted in the formation of larger EAAT2-immunoreactive clusters on the cell surface. The purified lipid raft-associated fractions were capable of Na^+-dependent glutamate uptake. Our data suggest that the glutamate transporters, especially EAAT2, are associated with cholesterol-rich lipid raft microdomains of the plasma membrane and that the association with these cholesterol-rich microdomains is important for excitatory amino acid transporter localization and function.

Glutamate is the major excitatory neurotransmitter used in the mammalian nervous system. Na^+-dependent excitatory amino acid transporters (EAATs)[1] are responsible for the uptake of glutamate as well as aspartate into the cell. Five mammalian Na^+-dependent excitatory amino acid transporters have been cloned to date: EAAT1 (GLAST), EAAT2 (GLT-1), EAAT3 (EAAC1), EAAT4, and EAAT5 (1). Within the nervous system, EAAT1 and EAAT2 are found primarily on astrocytes, whereas EAAT3 and EAAT4 are found principally on neurons (2–4). EAAT5 is expressed primarily in the retina (5). How are the expression and function of these transporters regulated? Stimulation of mouse cortical primary astrocyte cultures with glutamate increases the surface expression of EAAT1 (6). The expression and function of glutamate transporters can be regulated by activation of intracellular signaling molecules (7, 8). The function of glutamate transporters can also be modulated by interactions with other proteins. GTRAP3–18 interacts with and negatively modulates EAAT3-mediated glutamate transport (9, 10). GTRAP41 (β-spectrin-3) and GTRAP48 (RhoGEF-11) significantly increase EAAT4-mediated glutamate uptake (11).

Plasma membrane organization may be another means of regulating glutamate transporter function. Lipid rafts are lipid-protein microdomains of the plasma membrane that are enriched cholesterol and glycosphingolipids (12). These lipid raft microdomains have been implicated in regulating the trafficking and clustering of membrane-associated proteins as well as their intracellular signaling molecules. Lipid rafts are present on the surfaces of neurons as well as glial cells; many proteins of diverse functions including nicotinic acetylcholine receptors (13), α-amino-3-hydroxy-5-methylisoxazole-4-propanoic acid-type glutamate receptors (14, 15), metabotropic γ-aminobutyric acid receptors (16), glial cell-derived neurotrophic factor receptors (17), neural cell adhesion molecules (18), and SNARE proteins (19) have been shown to be associated with lipid rafts. Are glutamate transporters associated with these lipid raft microdomains? Proteoliposome reconstitution experiments have shown that cholesterol is required for Na^+-dependent [^{3}H]glutamate uptake (20). In addition, we have previously reported that Na^+-dependent [^{3}H]glutamate uptake is significantly reduced by long term treatment with the cholesterol-depleting agent methyl-β-cyclodextrin (MeβCD) (21). These results suggest that membrane cholesterol is important for the function of glutamate transporters.

In this study, we investigated the role of membrane cholesterol in the function of glutamate transporters. We found that glutamate transporters are partially associated with novel cho-

* This work was supported by National Institutes of Health Grant MH598005. The costs of publication of this article were defrayed in part by the payment of page charges. This article must therefore be hereby marked "*advertisement*" in accordance with 18 U.S.C. Section 1734 solely to indicate this fact.

¶ Present address: Dept. of Molecular and Cellular Biochemistry, The Ohio State University, 333 Hamilton Hall, 1645 Neil Ave., Columbus, OH 43210.

‡‡ To whom correspondence should be addressed: Dept. of Neuroscience, The Ohio State University, 4198 Graves Hall, 333 West 10th Ave., Columbus, OH 43210-1239. Tel.: 614-688-5433; Fax: 614-688-8742; E-mail: lin.492@osu.edu.

[1] The abbreviations used are: EAAT, excitatory amino acid transporter; biotin-CTXβ, biotinylated cholera toxin β subunit; chol-MeβCD, cholesterol complexed with MeβCD; conA, concanavalin A; dbcAMP, dibutyryl cyclic AMP; DHK, dihydrokainic acid; DRM, detergent-resistant microdomain; GTRAP, glutamate transporter-associated protein; mAb, monoclonal antibody; MeβCD, methyl-β-cyclodextrin; MES, 2-(N-morpholino)ethanesulfonic acid; pAb, polyclonal antibody; PBS, phosphate-buffered saline; PMV, plasma membrane vesicle; BSA, bovine serum albumin; SNARE, soluble NSF attachment protein receptors.

lesterol-rich, lipid raft-containing microdomains of the plasma membrane. EAAT2 is more strongly associated with these types of lipid rafts than the other glutamate transporters expressed in the brain. Furthermore, the association with these cholesterol-rich microdomains is important for EAAT localization and function.

EXPERIMENTAL PROCEDURES

Reagents—Methyl-β-cyclodextrin (MeβCD; mean degree of substitution = 10.5–14.7), cholesterol complexed with MeβCD (chol-MeβCD; 44 mg cholesterol/g solid), and biotinylated cholera toxin β subunit (biotin-CTXβ) were obtained from Sigma-Aldrich. Brij-58 (Surfact-Amps 58), EZ-Link Sulfo-NHS-SS-biotin, immobilized NeutrAvidin, Coomassie Plus Protein Assay, and SuperSignal West Pico chemiluminescent substrate were obtained from Pierce. The following antibodies were used in this study (the positions of the peptides used to generate each of these antibodies are given in parentheses): rabbit anti-EAAT1 pAb (positions 3–15 of rat EAAT1) (2), rabbit anti-EAAT2 pAb (positions 553–568 of human EAAT2) (2), rabbit anti-EAAT3 pAb (positions 510–523) (2), rabbit anti-EAAT4 pAb (positions 549–565 of human EAAT4) (22), chicken anti-GTRAP3–18 pAb (positions 1–188 of rat GTRAP3–18) (10), rabbit anti-GTRAP41 (β-spectrin-3) pAb (positions 2187–2201) (11), rabbit anti-GTRAP48 (RhoGEF-11) pAb (positions 38–52) (11), mouse anti-transferrin receptor mAb (clone H68.4), mouse anti-β-actin mAb (clone AC-40), or mouse anti-flotillin-1 mAb (clone 18). The mouse anti-β-actin mAb was obtained from Sigma-Aldrich, the mouse anti-flotillin-1 mAb was from BD Biosciences (San Diego, CA), the mouse anti-transferrin receptor mAb was from Zymed Laboratories Inc. (San Francisco, CA), and the rabbit pAbs directed against EAAT1, EAAT2, and EAAT4 as well as GTRAP41 and GTRAP48 were generously provided by Dr. Jeffrey D. Rothstein. Alexa Fluor 488 goat anti chicken IgG, Alexa Fluor 594 goat anti-chicken IgG, Alexa Fluor 594 goat anti-rabbit IgG, Alexa Fluor 488 avidin, and Amplex Red cholesterol assay kit were obtained from Molecular Probes (Eugene, OR). Unless otherwise stated, all other reagents were obtained from standard commercial sources.

Rat Primary Cortical Cultures—Neurons and astrocytes were cultured from newborn (12–24 h) rat cortices. The cortices were dissected out of the brains, incubated in activated papain for 30 min at 37 °C, triturated by repeated pipetting with a small bore pipette, and plated onto poly-D-lysine-coated (1 mg/ml) plastic culture dishes or glass slides. These cultures were maintained in Dulbecco's modified Eagle medium (Invitrogen) containing 25 mM glucose, 1 mM sodium pyruvate, 19.4 μM pyridoxine hydrochloride, 2 mM glutamine, 0.5% fetal bovine serum (Invitrogen), and 1% B-27 supplement (Invitrogen).

Plasma Membrane Vesicle Isolation—Adult male mouse forebrains were homogenized in 10 volumes homogenization buffer (320 mM sucrose in 50 mM Tris-HCl, pH 7.4) using a Dounce homogenizer (20 passes with a type B pestle) followed by a 23-gauge needle (5 passes). The homogenates were then centrifuged at 1000 × *g* for 10 min at 4 °C. The resultant supernatant (S1) was then centrifuged at 20,000 × *g* for 30 min at 4 °C. The plasma membrane vesicle (PMV) pellet (P2) was then resuspended in Na^+-containing or Na^+-free Kreb's buffer.

Discontinuous Sucrose Density Gradient Centrifugation—Adult male mouse brains were homogenized in 10 volumes of buffer A (150 mM NaCl, Complete protease inhibitor mixture (Roche Applied Science), 100 μM phenylmethylsulfonyl fluoride in 25 mM MES, pH 6.5, or buffer B (150 mM choline chloride, Complete protease inhibitor mixture (Roche Applied Science), 100 μM phenylmethylsulfonyl fluoride in 25 mM MES, pH 6.5) using a Dounce homogenizer (20 passes with a type B pestle) followed by a 23-gauge needle (5 passes). For the high salt fractionations, the concentration of NaCl in buffer A was adjusted to 1 M. The homogenates (diluted to 3 mg/ml protein) were then incubated with 1% (v/v) Triton X-100, 1% (v/v) Brij-58, or 1% (v/v) Lubrol WX for 60 min at 4 °C, after which sucrose was added to the samples to give a final concentration of 40% (w/v). 1 ml of each sample was overlaid with 1.8 ml of 30% (w/v) sucrose followed by 1.2 ml of 5% (w/v) sucrose and centrifuged for 16 h at 175,587 × *g* at 4 °C using a SW60 rotor (Beckman Coulter) and a L8-M Ultracentrifuge (Beckman Coulter). Ten 400-μl fractions were taken from each sample, and the pellet was resuspended in 400 μl of buffer (fraction 11).

Cellular Cholesterol Assay—The cells were lysed in reaction buffer (5 mM cholic acid, 0.1% Triton X-100 in PBS, pH 7.4) for 30 min at 4 °C and then sonicated. The membrane cholesterol was measured using the Amplex Red cholesterol assay kit according to the manufacturer's directions except that cholesterol esterase was omitted from the reaction mixture. Fluorescence was measured with a GENios microplate reader (Tecan Company; λ_{ex} = 545 nm, λ_{em} = 610 nm). The protein concentrations of the samples were determined using a Coomassie Plus protein assay according to the manufacturer's directions. The membrane cholesterol levels are expressed as specific fluorescence/mg protein.

Glutamate Uptake Assay—Uptake of radiolabeled glutamate was monitored in cells as described previously (10). Briefly, cultured cells grown on six-well plates were washed with 50 mM Tris-HCl and 320 mM sucrose, pH 7.4, and then incubated for 10 min at 37 °C with 10.2 nM L-[^{3}H]glutamate (0.5 μCi; Amersham Biosciences) in either Na^+-containing or Na^+-free Kreb's buffer supplemented with 40 μM unlabeled glutamate. The cells were washed with ice-cold PBS and then lysed in 1 mM NaOH. To distinguish dihydrokainic acid (DHK)-sensitive [^{3}H]glutamate uptake from DHK-insensitive uptake, samples were incubated with 300 μM DHK (Sigma-Aldrich) 30 min prior to uptake.

For measuring the uptake of [^{3}H]glutamate into PMVs, P2 fractions were resuspended in either Na^+-containing or Na^+-free Kreb's buffer, and 40 μg of synaptosomal protein sample were used in each assay. The samples were incubated in an equal volume of Na^+-containing or Na^+-free Kreb's buffer containing 10 μM L-glutamate supplemented with 2.04 nM L-[^{3}H]glutamate (0.1 μCi/ml) for 4 min at 37 °C and then rapidly chilled on ice. The chilled samples were passed through Whatman glass microfiber filters, and the filters were then washed twice with ice-cold PBS. The filters were then placed into scintillation mixture (ScintiSafe Econo 1; Fisher) and incubated overnight with shaking prior to counting. [^{3}H]glutamate uptake into DRMs and non-DRMs was accomplished as described above for uptake into PMV preparations except that 200 μl of each fraction was used per assay.

The amount of radiolabeled glutamate was measured using a Beckman Coulter LS6500 multi-purpose scintillation counter (Beckman Instruments). The conversion of scintillation counts to fmol [^{3}H]glutamate has been described previously (10). Na^+-dependent [^{3}H]glutamate uptake was calculated by subtracting Na^+-independent [^{3}H]glutamate uptake (in Na^+-free Kreb's buffer or buffer B for DRMs/non-DRMs) from the total [^{3}H]glutamate uptake (in Na^+-containing Kreb's buffer or buffer A for DRMs/non-DRMs). The protein concentrations of the samples were determined using a Coomassie Plus protein assay according to the manufacturer's directions. Na^+-dependent [^{3}H]glutamate uptake was expressed as fmol [^{3}H]glutamate/mg protein/min.

Lipid Raft Clustering—Cells grown on glass coverslips were incubated with 100 μg/ml biotin-CTXβ in PBS with 1% BSA for 60 min at 4 °C and then with Alexa Fluor 488-conjugated avidin (1:100) in PBS with 1% BSA for 60 min at 4 °C. The cells were then fixed and processed for immunofluorescence.

Immunofluorescence—Cells that were grown on glass coverslips were fixed with 2% paraformaldehyde, 50 mM sucrose, 400 mM $CaCl_2$ in 100 mM phosphate buffer for 30 min at room temperature followed by thorough rinsing with PBS+ (0.1% saponin, 0.02% sodium azide in PBS). The coverslips were then blocked with PBS with BSA (10 mg/ml BSA in PBS+) for 30 min at room temperature and then incubated with primary antibody solution (chicken anti-GTRAP3–18 pAb (1:500), rabbit anti-EAAT2 pAb (1:500), or rabbit anti-EAAT3 pAb (1:500) in PBS with BSA) overnight at room temperature. After rinsing, the coverslips were then incubated with secondary antibody solution (Alexa Fluor 488 goat anti chicken IgG (1:1000), Alexa Fluor 594 goat anti-chicken IgG (1:1000), or Alexa Fluor 594 goat anti-rabbit IgG (1:1000) in PBS with BSA) for 60 min at room temperatures. The coverslips were then rinsed and mounted onto glass slides with ImmuMount (Shandon Lipshaw).

Microscopy and Image Analysis—The images were obtained using a Zeiss 510 META Laser Scanning confocal microscope (Carl Zeiss Inc., Thornwood, NY) using either a 40× (NA = 1.3) or 100× (NA = 1.4) oil objective. A zoom factor of 6 was used for the images obtained with the 40× objective, whereas those obtained with the 100× objective were obtained with a zoom factor of 2. Optical sections were taken through the *z* axis of each cell at a thickness of 300 nm/section. For quantitative analysis of cluster characteristics, the images were obtained from an Axioskop 2 (Carl Zeiss) inverted microscopy with a 40× objective (numerical aperture, 0.75) using AxioVision 3.1. A collection of 20 slices (0.5 μm/slice) through the *z* plane were obtained for each image and were deconvolved using the regularized inverse filter algorithm. The following parameters were measured from the images: number of clusters, sectional area of the cell (μm^2), area of the clusters (μm^2), and intensity of the clusters (gray). Cluster density is defined by the following equation: cluster density (clusters/μm^2) = (number of clusters)/(sectional area). Unit cluster area is defined by the following equation: unit cluster area (μm^2/cluster) = (mean cluster area)/(number of clusters). Unit cluster intensity is defined by the following equation: unit cluster intensity (gray/μm^2) = (mean cluster intensity)/(mean cluster area).

Cell Surface Biotinylation—Labeling of proteins on the plasma membrane was accomplished by cell surface biotinylation as described previously (23). The cells were washed twice with PBS/CaMg (100 μM $CaCl_2$ and 1 mM $MgCl_2$ in PBS, pH 7.4) at room temperature and then incubated with biotinylation buffer (1 mg/ml EZ-Link Sulfo-NHS-SS-biotin in PBS/CaMg) for 20 min at 4 °C with constant shaking. The cells were then incubated with quenching buffer (100 mM glycine in PBS/CaMg) for 45 min at 4 °C with constant shaking and then incubated with lysis buffer (1% Triton X-100 and Complete protease inhibitor mixture (Roche Applied Science) in PBS, pH 7.4) for 30 min at 4 °C with constant shaking. The biotinylated proteins were recovered by incubation with 100 μl of immobilized NeutrAvidin (50% slurry) at 4 °C overnight with end-over-end rotation. The avidin beads were recovered by centrifugation (12,000 × *g* for 5 min at 4 °C) and then washed four times with Lysis buffer. After washing, the beads were resuspended in 1×SDS-PAGE sample loading dye (1.7% SDS, 6% glycerol, 100 mM dithiothreitol, 0.002% bromphenol blue in 50.3 mM Tris-HCl, pH 6.8).

Immunoblot Analysis—SDS-PAGE and electrotransfer of protein extracts was completed as described previously (10). The following primary antibodies were used: rabbit anti-EAAT1 pAb (1:200), rabbit anti-EAAT2 pAb (1:2000), rabbit anti-EAAT3 pAb (1:300), rabbit anti-EAAT4 pAb (1:200), chicken anti-GTRAP3–18 pAb (1:2500), rabbit anti-GTRAP41 pAb (1:200), rabbit anti-GTRAP48 pAb (1:100), mouse anti-β-actin mAb (1:500), mouse anti-transferrin receptor mAb (1:2000), or mouse anti-flotillin-1 mAb (1:250). The immunoreactive bands were detected using the SuperSignal West Pico chemiluminescent substrate according to the manufacturer's directions. Band intensities were measured using the Scion Image release Beta 4.0.2 (Scion Corporation, Frederick, MD).

Data Analysis and Statistical Analysis—The quantitative data are expressed as the means ± S.E. One-way analysis of variance was performed using Microsoft Excel 2002. Linear regression analysis was performed using SigmaPlot 2000 for Windows version 6.00 (SPSS Inc., Chicago, IL).

RESULTS

Depletion of Membrane Cholesterol Results in Reduced Glutamate Uptake in Primary Cortical Cultures—We previously found that Na^+-dependent [^{3}H]glutamate uptake was significantly reduced by treatment with 252 μM MeβCD, a cholesterol-depleting agent, for 4 days (21). To further investigate the role of cholesterol in the function of glutamate transporters, we examined the effect of transient exposure to 10 mM MeβCD. This dosage has been often used in cholesterol depletion experiments (24). Rat primary cortical cultures were used in this study. Our cultures primarily contained neurons, which expressed EAAT3, and type II astrocytes, which expressed EAAT2, as determined by immunostaining (data not shown). The cultures were treated with10 mM MeβCD for 3 and 30 min and then assessed for changes in [^{3}H]glutamate uptake and membrane cholesterol content. The cultures were also treated with an equivalent amount of MeβCD complexed with cholesterol (chol-MeβCD; 1.5 mM cholesterol in 10 mM MeβCD) so as to determine whether the observed MeβCD-induced effects would be the result of cholesterol depletion. The cell number and the cell morphology were not visibly altered after these treatments. Na^+-dependent [^{3}H]glutamate uptake was significantly reduced by 64.5 ± 2.5% (n = 3; p = 0.00035) and 98.2 ± 0.1% (n = 3; p = 0.000029) in cultures exposed to MeβCD for 3 and 30 min, respectively; however, there was no significant change in the chol-MeβCD-treated cultures at 3 min, and [^{3}H]glutamate uptake was increased by 23.1 ± 11.8% (n = 3; p = 0.071) at 30 min as compared with vehicle (Fig. 1*A*). Membrane cholesterol levels were significantly reduced in the MeβCD-treated cultures (60.5 ± 1.3% decrease at 3 min (n = 3; p = 0.000004) and 88.2 ± 2.0% decrease at 30 min (n = 3; p = 0.0004)) and were increased in the chol-MeβCD-treated cultures (13.9 ± 10.2% increase at 3 min (n = 3; p = 0.057) and 16.4 ± 11.6% increase at 30 min (n = 3; p = 0.076)) as compared with vehicle (Fig. 1*B*). Regression analysis revealed a linear relationship (R^2 = 0.9434) between membrane cholesterol levels and Na^+-dependent [^{3}H]glutamate uptake upon exposure to MeβCD.

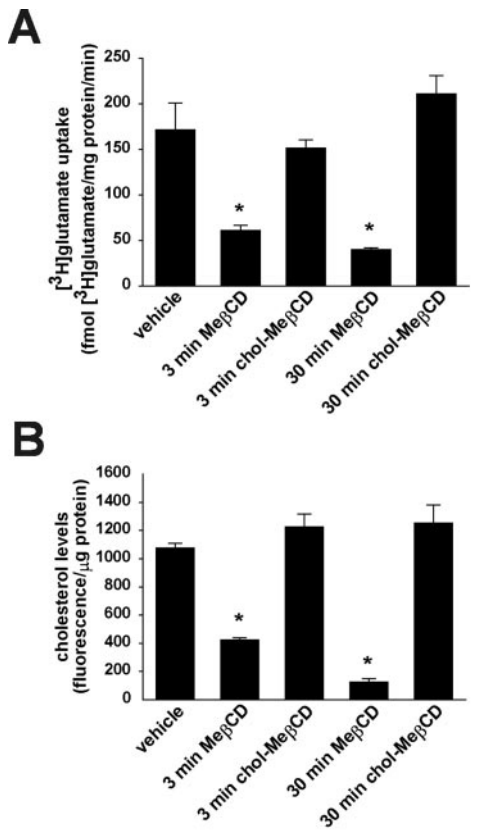

FIG. 1. **The effect of cholesterol depletion by MeβCD on glutamate uptake in rat primary cortical cultures.** Rat cortical cultures were incubated with either 10 mM MeβCD or an equivalent amount of chol-MeβCD for 3 or 30 min and then assayed for Na^+-dependent [^{3}H]glutamate uptake and membrane cholesterol content. *A*, MeβCD significantly reduced Na^+-dependent [^{3}H]glutamate uptake with increasing incubation time (*, $p < 0.0005$). Na^+-dependent [^{3}H]glutamate uptake was not significantly altered by treatment with chol-MeβCD when compared with vehicle-treated cultures (n = 3/group). *B*, MeβCD significantly reduced membrane cholesterol levels in a time-dependent manner (*, $p < 0.000005$), whereas chol-MeβCD complex did not significantly alter the membrane cholesterol content (n = 3/group).

To examine the effect of cholesterol depletion on different glutamate transporter subtypes, DHK (300 μM) was used to distinguish EAAT2-mediated glutamate uptake from uptake mediated by the other EAATs because DHK has a higher affinity for EAAT2 (25). We found that DHK-sensitive uptake was more profoundly affected by cholesterol depletion (reduced by 47.1 ± 10.1% n = 3; p = 0.040) than DHK-insensitive uptake (reduced by 17.4 ± 1.5%, n = 3; p = 0.011) after 3 min of exposure to MeβCD. These results indicated that depletion of membrane cholesterol results in reduced Na^+-dependent glutamate transport, and EAAT2-mediated glutamate uptake appears more sensitive to this effect.

Depletion of Membrane Cholesterol Alters the Membrane Distribution of EAAT2 and EAAT3—What are the mechanisms responsible for the decrease in Na^+-dependent glutamate uptake observed in MeβCD-treated cortical cultures? We examined total EAAT2 and EAAT3 protein levels by immunoblot analyses. There was no change in EAAT2 protein level. For unknown reasons, EAAT3 protein could not be detected in these cell extracts by immunoblot analysis, but immunostaining showed no visible change in total intensity (see below). We then examined whether MeβCD alters the cell surface EAAT2 level using cell surface biotinylation assays. As shown in Fig. 2*A*, there was a decrease in the amount of surface (*i.e.*

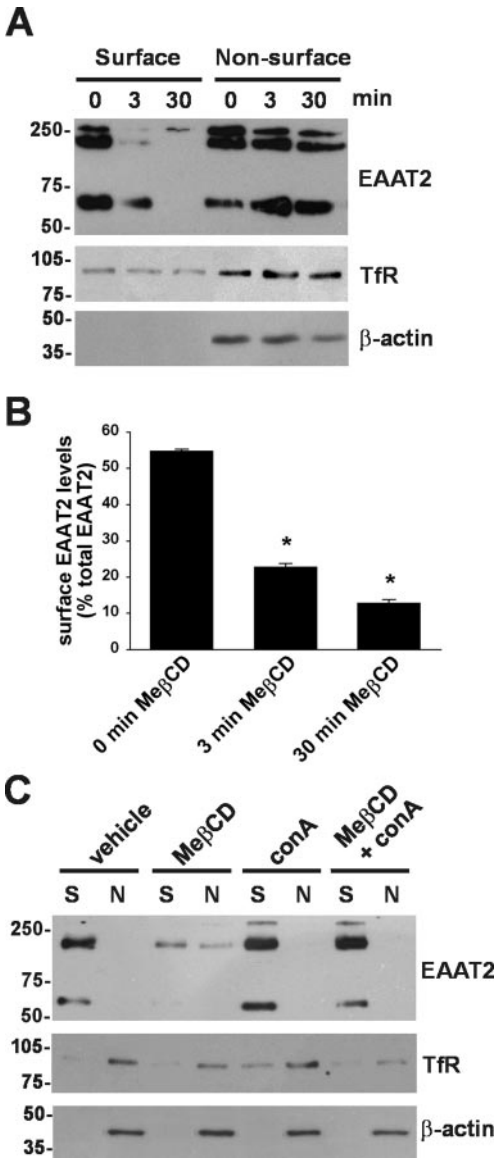

FIG. 2. **The effect of MeβCD on the surface expression of EAAT2 in rat primary cortical cultures.** *A*, avidin-bound protein extracts (50% of total volume) as well as equivalent volumes of avidin-unbound protein extracts (10% of total volume) from rat primary cortical cultures treated with 10 mM MeβCD for 3 or 30 min were analyzed for EAAT2, transferrin receptor, and β-actin by immunoblot. Vehicle-treated samples are designated as *0 min lanes*. MeβCD treatment reduces cell surface EAAT2 (*i.e.* avidin-bound) levels and increases intracellular EAAT2 (*i.e.* avidin-unbound) levels. MeβCD, however, did not affect the surface expression of transferrin receptor. *B*, quantitation of surface EAAT2 band intensity in MeβCD-treated and untreated samples. The sum intensity of the EAAT2 bands in the avidin-bound and unbound lanes were normalized to that of the β-actin band. The surface EAAT2 levels were expressed relative to total EAAT2 band intensity. MeβCD significantly reduced surface EAAT2 levels in a time-dependent manner ($n = 3$/group). *, $p < 0.000002$. *C*, effect of membrane internalization inhibition by conA on the MeβCD-induced reduction in surface EAAT2 levels. Primary cortical cultures were treated for 30 min with either 10 mM MeβCD, 250 μg/ml conA, or 10 mM MeβCD + 250 μg/ml conA and subjected to cell surface biotinylation assays. Aliquots of cell surface (*S*; *i.e.* avidin-bound) and nonsurface (*N*; avidin-unbound) protein extracts were analyzed for EAAT2 levels by immunoblot as described above. Co-incubation with conA prevented the reduction in surface (*S*) EAAT2 caused by MeβCD treatment.

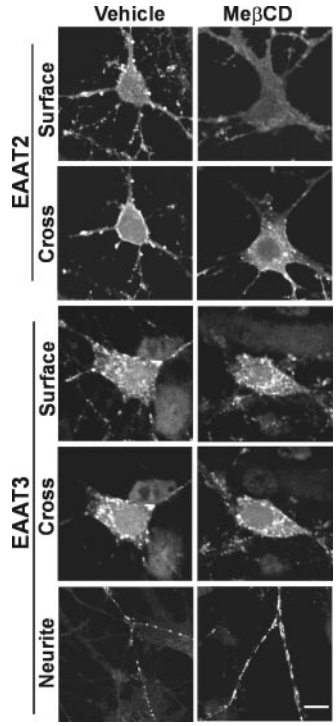

FIG. 3. **The effect of MeβCD on the plasma membrane localization of EAAT2 and EAAT3.** Rat primary cortical cultures were treated with either vehicle (PBS) or 10 mM MeβCD for 3 min and processed for immunofluorescent staining. The clustered distribution of EAAT2 was disrupted on the cell surface by MeβCD (*Surface*). MeβCD reduced the amount of EAAT2 present on the surface and increased the amount of intracellular EAAT2 (*Cross*). The punctate distribution of EAAT3 across the surface of the neuronal cell body was dispersed by MeβCD. Additionally, the amount of intracellular EAAT3 staining increased in MeβCD-treated cells relative to untreated cells (*Cross*). MeβCD also altered the distribution and trafficking of EAAT3 to neuronal processes (*Neurite*). *Scale bar*, 10 μm.

biotinylated) EAAT2 levels and a coordinate increase in the amount of nonsurface (*i.e.* nonbiotinylated) EAAT2 levels in the cultures treated with 10 mM MeβCD in a time-dependent manner as revealed by immunoblot analysis. MeβCD did not affect the amount of the membrane protein transferrin receptor protein present on the cell surface (Fig. 2*A*). As a specificity control, the intracellular protein β-actin was only found in the nonsurface fractions. Quantitative analysis of immunoreactive bands (*i.e.* EAAT2 band intensities normalized to those for β-actin) revealed that MeβCD reduced surface EAAT2 expression by 58.4 ± 1.8% ($n = 3$, $p = 0.0000012$) and 76.7 ± 1.8% ($n = 3$, $p = 0.00000038$) after 3 and 30 min of exposure, respectively (Fig. 2*B*).

MeβCD-induced reduction in surface EAAT2 may result from increased endocytosis of EAAT2 present on the cell surface. We examined the effect of inhibition of receptor internalization on the MeβCD-induced reduction in surface EAAT2 by co-treating primary cortical cultures with 10 mM MeβCD and 250 μg/ml concanavalin A (conA), a nonspecific inhibitor of receptor internalization (26), for 30 min. The amount of surface EAAT2 protein is greater in cells treated with MeβCD and conA than those treated with MeβCD alone (Fig. 2*C*), suggesting that receptor-mediated endocytosis may be involved in the MeβCD-induced reduction in surface EAAT2.

Immunostaining followed by confocal microscopy was performed to examine the effect of MeβCD on the localization of EAAT2 and EAAT3. As shown in Fig. 3, EAAT2 was primarily localized on the plasma membrane in discreet clusters in vehicle-treated astrocytes; however, the clusters appeared to disperse in the astrocytes treated with 10 mM MeβCD for 3 min (compare EAAT2 surface micrographs). Furthermore, a reduction in the intensity of EAAT2 staining on the cell surface with an increase in intracellular EAAT2 immunolabeling was observed (compare EAAT2 cross-micrographs). Quantitative

analysis of cluster characteristics using deconvolution microscopy and image analysis showed a 26.4 ± 4.4% reduction (p = 0.014) in cluster number, a 21.2 ± 4.5% reduction (p = 0.025) in cluster size, and a 61.5 ± 0.3% reduction (p = 0.000011) in cluster intensity on cells treated with MeβCD as compared with vehicle-treated cells (n = 10). These results suggest that depletion of membrane cholesterol reduces the localization of the EAAT2 to the cell surface and may also alter the clustering of EAAT2 on the plasma membrane. EAAT3 was localized on the plasma membrane and cytoplasm within the neuronal cell body in discreet clusters in vehicle-treated neurons. A slight reduction in the intensity of EAAT3 staining on the cell surface was observed in the neurons treated with 10 mM MeβCD for 3 min. Quantitative analysis of cluster characteristics showed no significant change in cluster number and cluster size but a 27.1 ± 3.0% reduction (p = 0.054) in cluster intensity on cells treated with MeβCD as compared with vehicle-treated cells (n = 10). Furthermore, EAAT3 immunostaining was concentrated in larger clusters within the neurites (presumably dendrites) of neurons treated with MeβCD (EAAT3 neurite micrographs in Fig. 3). These results suggest that MeβCD may also affect the membrane localization and distribution of EAAT3, but these effects are less when compared with EAAT2.

MeβCD Reduces Glutamate Transporter Function in Plasma Membrane Vesicles by Removing Cholesterol—The loss of EAAT2 on the cell surface does not temporally correlate with the reduction in EAAT2-mediated [^{3}H]glutamate uptake (compare Figs. 2*B* and 1*A*), suggesting that cholesterol may be essential for glutamate transporter function on the plasma membrane. We investigated whether MeβCD had effect on the glutamate uptake of PMVs that were prepared from mouse forebrains. This allowed us to determine the effect of cholesterol depletion on the plasma membrane without the influences of membrane protein trafficking. PMVs contain neuron synaptosomal vesicles as well as glial plasmalemmal vesicles, both of which are capable of Na^+-dependent glutamate uptake (27). PMVs were treated with either MeβCD (10 mM), chol-MeβCD (1.5 mM cholesterol in 10 mM MeβCD), or vehicle (PBS) for 30 min at 4 °C and then assayed for [^{3}H]glutamate uptake and membrane cholesterol content. MeβCD reduced Na^+-dependent [^{3}H]glutamate uptake by 59.3 ± 3.4% (n = 3; p = 0.0042) and chol-MeβCD increased uptake by 28.3 ± 7.9% (n = 3; p = 0.025) when compared with the vehicle-treated PMVs (Fig. 4*A*). MeβCD also reduced membrane cholesterol content by 14.8 ± 2.2% (n = 3; p = 0.0064) and chol-MeβCD increased cholesterol levels by 10.2 ± 0.5% (n = 3; p = 0.0017) when compared with vehicle (Fig. 4*B*). Regression analysis revealed a linear relationship (R^2 = 0.9961) between cholesterol levels and Na^+-dependent [^{3}H]glutamate uptake. Furthermore, MeβCD or chol-MeβCD had no significant effect of DHK-insensitive uptake. MeβCD significantly decreased DHK-sensitive uptake by 88.1 ± 3.6% (n = 3; p = 0.0024) and chol-MeβCD increased DHK-insensitive uptake by 48.4 ± 1.4% (n = 3; p = 0.0056) (Fig. 4*C*). These results indicate that the ability of EAAT2 to function properly on the cell surface may depend on its association with cholesterol.

Glutamate Transporters Are Associated with Cholesterol-enriched Microdomains of the Plasma Membrane—The above results suggest that the organization of functional glutamate transporter complexes, especially those containing EAAT2, may be regulated by the membrane cholesterol. Cholesterol is enriched in discreet lipid-protein microdomains of the plasma membrane known as lipid rafts (28). The rafts can be isolated from the rest of the plasma membrane by their flotation in discontinuous sucrose gradients based on their detergent insolubility at low temperature. These plasma membrane domains

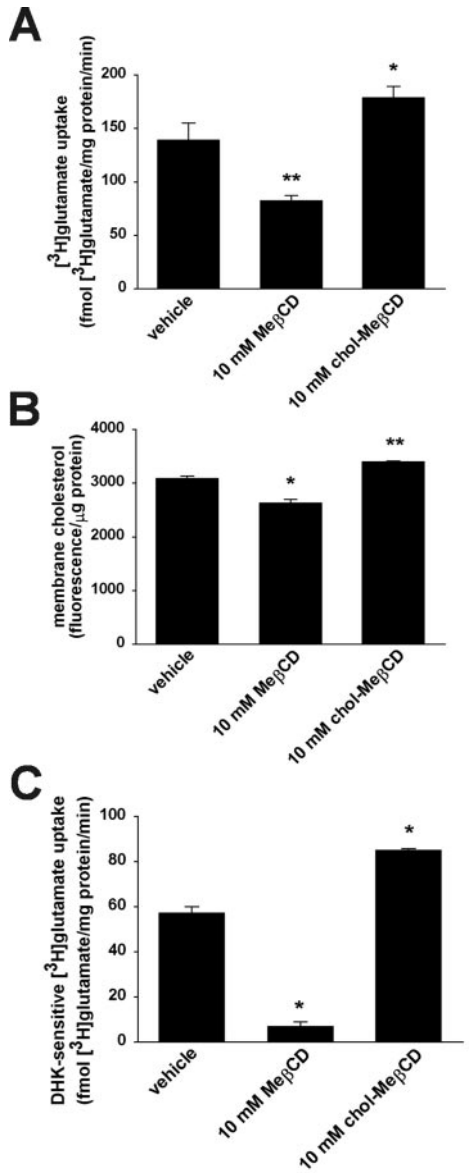

FIG. 4. **The effect of MeβCD and chol-MeβCD on glutamate uptake in mouse brain PMVs.** Mouse forebrain PMVs were treated with 10 mM MeβCD or an equivalent amount of chol-MeβCD for 30 min at 4 °C and then analyzed for Na^+-dependent [^{3}H]glutamate uptake and membrane cholesterol content. *A*, MeβCD significantly reduced Na^+-dependent [^{3}H]glutamate uptake in mouse forebrain PMVs. chol-MeβCD increased Na^+-dependent [^{3}H]glutamate uptake in mouse forebrain PMVs (n = 3/group). *, $p < 0.05$; **, $p < 0.005$. *B*, MeβCD reduced membrane cholesterol levels in mouse forebrain PMVs, whereas chol-MeβCD increased vesicular cholesterol content. (n = 3/group). *, $p < 0.005$; **, $p < 0.002$. *C*, MeβCD significantly reduced DHK-sensitive, Na^+-dependent [^{3}H]glutamate uptake in mouse forebrain PMVs, whereas chol-MeβCD increased DHK-sensitive, Na^+-dependent [^{3}H]glutamate uptake in mouse forebrain PMVs (n = 3/group). *, $p < 0.05$.

have been, therefore, called detergent-resistant microdomains (DRMs) (12). Triton X-100 has been the nonionic detergent most commonly used for these analyses. However, not all proteins that are associated with lipid raft microdomains are insoluble in Triton X-100. Some proteins that are associated with lipid raft microdomains, such as prominin, are soluble in Triton X-100 but insoluble in more hydrophilic nonionic detergents such as Brij-58 and Lubrol WX (29). We investigated whether glutamate transporters are associated with DRMs prepared under different detergent solubilization conditions. Mouse forebrain homogenates were solubilized with 1% Triton X-100, 1%

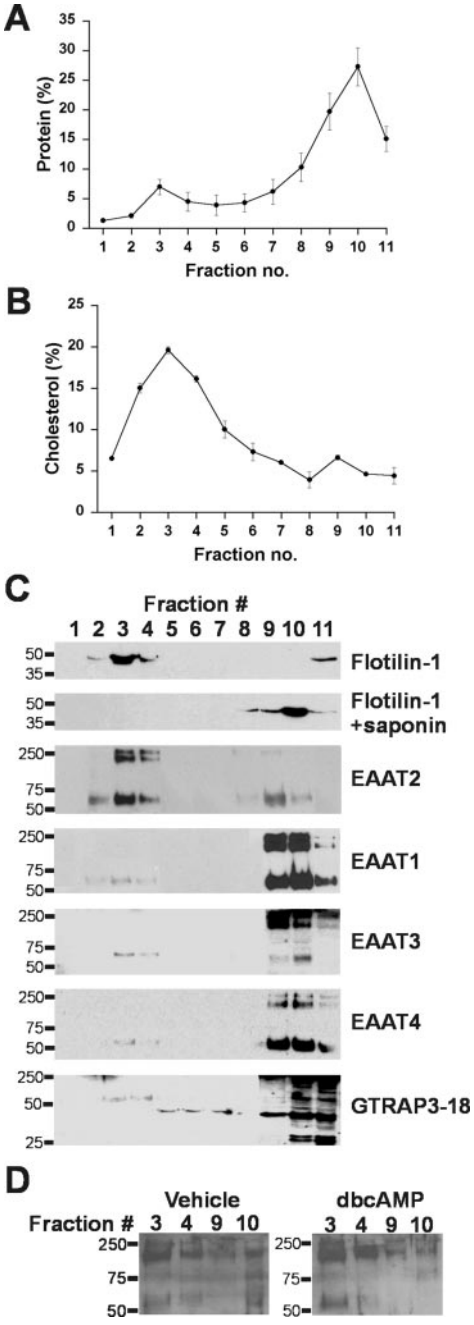

FIG. 5. **The localization of EAATs and their regulatory proteins to detergent insoluble, lipid raft microdomains.** Mouse forebrain extracts were solubilized in 1% Brij-58 and fractionated through a discontinuous sucrose gradient. Protein (*A*) and cholesterol (*B*) levels were measured in each of the fractions. Most of the protein present in the samples were found in the high density fractions (*fractions 8–11*). A relatively high cholesterol content was observed in the low density fractions (*fractions 2–4*). *C*, fractionation profiles for the EAATs and the EAAT3-interacting protein GTRAP3–18 following Brij-58 solubilization. Flotillin-1, a marker protein for lipid raft-containing fractions, was present primarily in fractions 2–4; therefore, fractions 2–4 are defined as the DRM-containing fractions. The specificity for the localization of flotillin-1 to DRM-containing fractions was demonstrated using the lipid raft-disrupting detergent saponin (0.5%) during solubilization. A large portion of EAAT2 and a small portion of EAAT1, EAAT3, and EAAT4 were detected in the DRM-containing fractions (*fractions 2–4*) following Brij-58 solubilization. A minor amount of total GTRAP3–18 multimers was also present in the Brij-58-solubilized DRM-containing fractions. *D*, effect of dbcAMP on the fractionation profile of EAAT2. dbcAMP (250 μM for 30 min) increased the amount of EAAT2 protein present in the DRM-containing fractions (*fractions 3* and *4*) in primary rat cortical cultures. Interestingly, dbcAMP also decreased the amount of EAAT2 present in the high density, non-DRM-containing fractions (*fractions 9* and *10*).

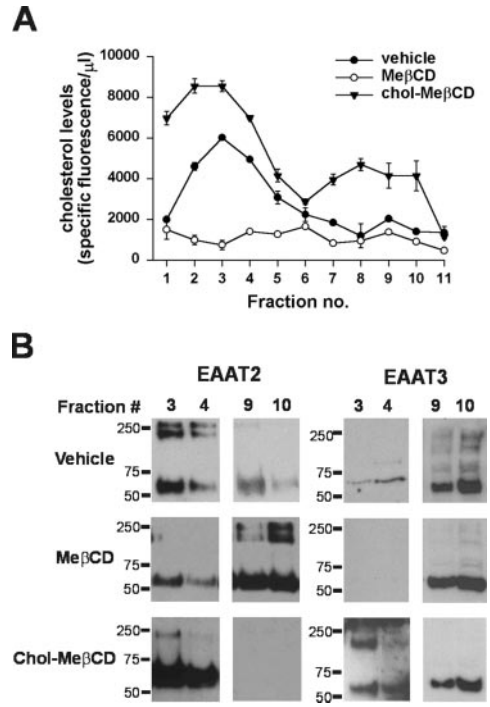

FIG. 6. **The dependence of lipid raft association of EAAT2 and EAAT3 on cholesterol.** Mouse forebrain extracts were treated with MeβCD or chol-MeβCD at 4 °C prior to solubilization with Brij-58 and fractionation through a discontinuous sucrose gradient. *A*, cholesterol levels in fractions 2–4 were reduced following treatment with MeβCD and were increased upon exposure to chol-MeβCD. *B*, MeβCD reduced the amount of EAAT2 and EAAT3 in the DRM-containing fractions (*fractions 3* and *4*) when compared with vehicle. Chol-MeβCD, on the other hand, increased the amount of EAAT2 and EAAT3 present in fractions 3 and 4 as compared with vehicle and with MeβCD.

Brij-58, or 1% Lubrol WX at 4 °C and fractionated through a discontinuous sucrose gradient (5–30 to 40%). The DRMs and their associated proteins migrated to the upper, low density region of the gradient because of their high lipid content. Detergent-soluble materials remained in the lower, high density fractions, and the detergent-insoluble cytoskeletal components pellet at the bottom of the tube. The fractions were collected from the top of the gradient (*fractions 1–11*). About 80–90% of the protein was found in the high density fractions (*fractions 8–11*) with ~5–10% of protein was present in low density fractions (*fractions 2–4*) in all cases (Fig. 5*A*). Relatively high cholesterol content was found in the low density fractions (Fig. 5*B*, *fractions 2–4*). In the cases of both 1% Brij-58 and 1% Lubrol WX, the amount of protein and cholesterol in the low density fractions (*fractions 2–4*) was higher than in the case of solubilization with 1% Triton X-100. Flotillin-1, which is known to be associated with lipid rafts (30), was localized to fractions 2–4 (Fig. 5*C*). To further demonstrate the specificity of the localization of flotillin-1 to DRM fractions, Brij-58-solubilized samples were preincubated with 0.5% saponin, a nonionic detergent that disrupts protein-cholesterol interactions when used at this concentration (16), before fractionation. Flotilin-1 was found only in fractions 8–11 (Fig. 5*C*). These results indicated that fractions 2–4 contained lipid raft microdomains.

In the case of solubilization with 1% Triton X-100, virtually no glutamate transporters proteins (EAAT1–3) were detected in DRM fractions (data not shown). However, a large portion of total EAAT2 and a minor portion of total EAAT1 and EAAT3 were detected in DRM fractions (fractions 2–4) upon solubilization with 1% Brij-58 (Fig. 5*C*) or 1% Lubrol WX. The amounts of DRM-associated EAAT1–3 were similar between those lysates treated with Lubrol WX and those with Brij-58. We also

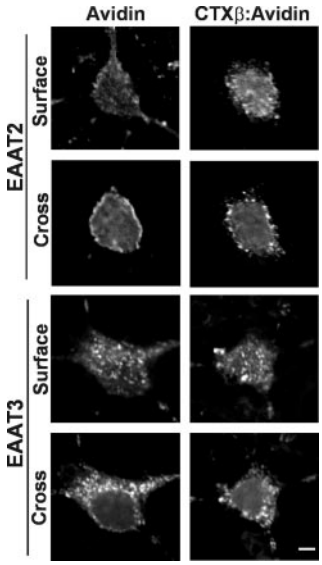

FIG. 7. **The effect of artificial patching of lipid rafts on the surface localization of EAAT2 and EAAT3.** Immunofluorescent staining for EAAT2 and EAAT3 was performed on rat cortical cultures that were treated either with biotin-CTXβ and avidin (*CTXβ:Avidin*) or avidin prior to fixation. The number and sizes of EAAT2-immunoreactive clusters on the surface increased in CTXβ:avidin-treated cells. The sizes of the EAAT3-immunoreactive clusters also increased upon patching with CTXβ:avidin and biotin but to a lesser extent than for EAAT2. *Scale bar*, 10 μm.

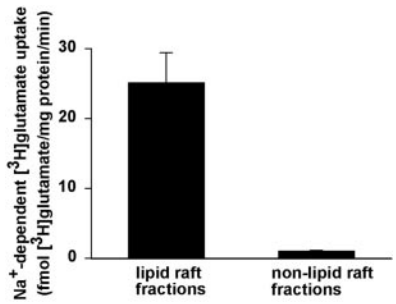

FIG. 8. **Na^+-dependent [^{3}H]glutamate uptake in low density, Brij-58 -resistant, lipid raft-containing vesicles from mouse forebrain extracts.** Na^+-dependent [^{3}H]glutamate uptake was measured in vesicles derived from lipid raft fractions (n = 3) and those derived from nonlipid raft fractions (n = 3) generated from resolving Brij-58 -solubilized mouse forebrain extracts through a discontinuous sucrose density gradient. Vesicles derived from DRM fractions were capable of Na^+-dependent [^{3}H]glutamate uptake, whereas those derived from non-DRM fractions did not show any appreciable Na^+-dependent [^{3}H]glutamate uptake.

examined whether EAAT4 is associated with Brij-58-resistant microdomains using mouse cerebellum homogenates. Like EAAT1 and EAAT3, a minor portion of total EAAT4 was localized to fractions 2–4 (Fig. 5*C*). To determine whether EAATs directly associated with DRMs, mouse forebrain homogenates were solubilized in 1% Brij-58 under conditions of high stringency (*i.e.* 1 M NaCl as compared with 120 mM NaCl). The amounts of DRM-associated EAATs were similar under highly stringent conditions relative to low stringency conditions (data not shown), indicating that the association of EAATs with lipid raft microdomains is both specific and direct. Furthermore, the amounts of EAATs associated with Brij-58-resistant microdomains were similar between forebrain, cerebellum, and spinal cord (data not shown).

The association of glutamate transporter-associated proteins to Brij-58-resistant microdomains was also examined in mouse brain homogenates. GTRAP3–18 interacts with EAAT3 (9), whereas GTRAP41 (β-spectrin-3) and GTRAP48 (RhoGEF-11) interact with EAAT4 (11). As shown in Fig. 5*C*, a minor portion of GTRAP3–18 multimers were present in the DRM-containing fractions (fractions 2–4). GTRAP41 and GTRAP48, however, were only found in the non-DRM-containing fractions (fractions 8–11; data not shown).

Long term treatment with dibutyryl cyclic AMP (dbcAMP) induces the expression, membrane localization, and function of EAAT2 in astrocytes as well as in neuron-astrocyte mixed cultures (31, 32). Does dbcAMP also affect the localization of EAAT2 to lipid raft microdomains? To answer this question, we treated rat cortical primary cultures with 250 μM dbcAMP (or vehicle) for a short period of time (30 min), solubilized the resultant extracts with 1% Brij-58, and fractionated the samples through a discontinuous sucrose density gradient. dbcAMP increased the amount of EAAT2 protein present in the DRM-containing fractions (*fractions 3* and *4*) and reduced the amount of EAAT2 in the high density, non-DRM-containing fractions (Fig. 5*D*, *fractions 9* and *10*). These experiments demonstrate that dbcAMP increases the membrane localization of EAAT2 in addition to inducing the expression and surface trafficking of EAAT2.

Is the association of EAAT2 and EAAT3 with DRM-containing fractions dependent on cholesterol? Mouse forebrain homogenates were treated with either 10 mM MeβCD or 10 mM chol-MeβCD (30 min at 4 °C) prior to Brij-58 solubilization and fractionation. Treatment of mouse forebrain extracts with MeβCD reduced the amount of cholesterol present in fractions 2–4 (Fig. 6*A*). The cholesterol content in fractions 2–4 was higher in extracts treated with chol-MeβCD than in vehicle-treated extracts. The amount of EAAT2 and EAAT3 in the DRM-containing fractions (*fractions 3* and *4*) was reduced in MeβCD-treated samples relative to vehicle-treated samples (Fig. 6*B*). Interestingly, the relative amounts of EAAT2 and EAAT3 present in the fractions 3–4 were higher in chol-MeβCD-treated samples relative to MeβCD-treated as well as vehicle-treated samples (Fig. 6*B*). These results suggest that the association of EAAT2 and EAAT3 with lipid raft microdomains is dependent on cholesterol.

Artificial Patching of Lipid Rafts Results in Co-patching of EAAT2—The aforementioned pharmacological, immunohistochemical, and biochemical experiments strongly suggest that EAATs, especially EAAT2, may be partially associated with cholesterol-rich lipid raft microdomains on the plasma membrane. Another way to demonstrate the association of EAATs with these lipid raft microdomains would be to artificially aggregate lipid rafts on the plasma membrane and determine whether the EAATs would also be aggregated (co-patching experiments). In these experiments, lipid raft microdomains were artificially aggregated by incubation of cells with biotinylated cholera toxin-β (biotin-CTXβ) and avidin prior to fixation and immunofluorescence. CTXβ has a strong affinity for G_M1 gangliosides, which are enriched in lipid raft microdomains (33). Rat primary cortical cultures were analyzed for EAAT2 and EAAT3 immunoreactivity after biotin-CTXβ:avidin aggregation. Aggregation of lipid rafts with biotin-CTXβ:avidin resulted in the formation of larger EAAT2-immunoreactive clusters on the cell surface (Fig. 7). EAAT3-immunoreactive clusters were also larger on biotin-CTXβ:avidin-patched cells than avidin-treated cells, but the degree of change was smaller for EAAT3 than for EAAT2 (Fig. 7). These results further support that EAAT2 is associated with the cholesterol-rich lipid raft on the plasma membrane.

The Lipid Raft Microdomains Are Capable of Glutamate Uptake—Is the association of EAATs with lipid raft microdomains required for functional glutamate transport? We exam-

ined Na^+-dependent [^{3}H]glutamate uptake in vesicles derived from DRM-containing and non-DRM-containing fractions generated from resolving Brij-58-solubilized mouse forebrain extracts through a discontinuous sucrose density gradient. The DRM-containing fractions (Fig. 5*C*, *fractions 2–4*) were capable of Na^+-dependent [^{3}H]glutamate uptake, whereas the vesicles derived from the non-DRM-containing fractions (Fig. 5*C*, *fractions 9–10*) possessed negligible Na^+-dependent [^{3}H]glutamate uptake activity (Fig. 8). The lack of Na^+-dependent [^{3}H]glutamate uptake in vesicles from non-DRM-containing fractions was not the result of the higher sucrose concentration because they were still not capable of uptake when the sucrose concentration was reduced to a concentration similar to that in the DRM-containing fractions. Moreover, it was also not due to higher Brij-58 concentration because the addition of 1% Brij-58 to DRM-containing vesicles did not significantly reduce uptake activity (data not shown). These results indicated that association of EAATs with cholesterol-rich lipid raft microdomains may be required for functional transport of glutamate.

DISCUSSION

In this study, we used biochemical, immunohistochemical, and pharmacological approaches to investigate the role of membrane cholesterol in the function of glutamate transporters. We found that a large portion of total EAAT2 is associated with cholesterol-rich lipid raft microdomains. The association with these cholesterol-rich microdomains is important for the trafficking of EAAT2 to the plasma membrane and the organization of functional complexes on the plasma membrane. Lipid rafts have been implicated in the regulation of numerous cellular events including membrane trafficking, membrane organization, and signal transduction (34–36). Our results suggest that glutamate transporters, especially EAAT2, are regulated by this mechanism.

Several lines of evidences indicate that the function of glutamate transporters is associated with membrane cholesterol. Proteoliposome reconstitution experiments have shown that cholesterol is required for Na^+-dependent glutamate uptake (20). Na^+-dependent glutamate uptake is significantly reduced by long term treatment with the cholesterol-depleting agent MeβCD (21). Glutamate transporters are organized on the plasma membrane of astrocytes and neurons in a clustered manner (4, 37, 38), and depletion of membrane cholesterol results in reduced cluster number and cluster size. Additionally, a recent study has demonstrated that glia-derived cholesterol regulates the activity and expression of the neuronal glutamate transporter EAAT3 (39).

The composition of lipid rafts is not homogeneous. Lipid rafts isolated from mouse brain plasma membrane vesicles using different means of isolation had different lipid and protein compositions (40). Lipid raft-associated associated proteins are classically defined by their insolubility in the nonionic detergent Triton X-100 under cold conditions (34); however, not all proteins that are associated with cholesterol-rich microdomains are insoluble in Triton X-100. The pentaspan membrane protein prominin is localized to cholesterol-rich domains of the plasma membrane of microvilli; however, prominin is soluble in Triton X-100 (29). The use of more hydrophobic nonionic detergents such as Lubrol WX and Brij-58 reduced the solubility of prominin (29). Interestingly, the EAATs are also soluble in Triton X-100 but not in Brij-58.

Not all of the EAATs expressed in the brain are associated with cholesterol-rich lipid raft microdomains to the same extent. EAAT2 is more strongly associated with Brij-58-insoluble, cholesterol-rich lipid raft microdomains than EAAT1, EAAT3, and EAAT4. There are many possible mechanisms that could account for the differential solubility of EAATs to Brij-58. Because EAAT2 is the primary glutamate transporter responsible for glutamate clearance in the central nervous system, and EAAT2 function depends on its association with cholesterol, the increased localization of EAAT2 to Brij-58-insoluble, cholesterol-rich microdomains may be a consequence of its constitutive activity near the synapse. Alternatively, the lipid composition of astrocyte plasma membrane may be different from that for neuronal plasma membranes so the differential association of EAAT2 and EAAT3 with cholesterol-rich microdomains may reflect differences in lipid raft composition. Future experiments designed at understanding the molecular basis of the association of the EAATs to cholesterol-rich, lipid raft-containing microdomains could provide novel insights into this issue.

Could the association with lipid raft microdomains regulate the trafficking of the EAATs from the trans-Golgi network to the plasma membrane? The rapsyn-mediated transport of nicotinic acetylcholine receptors to the cell surface is dependent on its association with lipid rafts (41). Chronic depletion of membrane cholesterol by MeβCD results in the intracellular accumulation of EAAT3 in HEK293 cells as well as in primary cultured neurons (21). In fact, the treatment of primary cortical cultures with 10 mM MeβCD for 30 min significantly reduces the surface expression of EAAT2 and EAAT3 as shown with cell surface biotinylation assays and immunofluorescence microscopy. It is possible that association of EAAT2 and EAAT3 with cholesterol-rich lipid rafts may regulate the trafficking of these transporters to the cell surface.

The polarized distribution of EAAT3 to the apical surface of Madin-Darby canine kidney cells and to the dendrites of primary hippocampal cultures is mediated through a sorting motif on the C terminus of EAAT3 (42). Could the dendritic sorting of EAAT3 be regulated by its association with cholesterol-rich lipid raft microdomains? In this study, the localization of EAAT3 to dendrites is altered by the depletion of cholesterol using MeβCD, suggesting that association of EAAT3 with cholesterol may be required for sorting to dendrites. Disruption of lipid raft-associated complexes in polarized hippocampal neurons results in the mis-sorting of axonal (apical) proteins but not those proteins localized to dendrites (43). This finding would discount the importance of association with cholesterol-rich microdomains in the sorting of EAAT3 to dendrites because lipid raft association affects axonal targeting. However, EAAT3 is unique in that it is localized to the apical membrane in kidney cells (44) but is present on somatodendritic processes of neurons (4), so lipid raft association may modulate the targeting of EAAT3 to dendrites. Further analysis could be conducted relating the lipid raft association of EAAT3 to dendritic sorting. Lipid raft-associated proteins that are Triton X-100-soluble but insoluble in Lubrol WX are sorted from the trans-Golgi network directly to the apical membrane of polarized HepG2 cells, but Triton X-100-insoluble lipid raft-associated proteins arrive at the apical membrane via transcytosis (45). This study underlies the importance of different types of lipid raft microdomains on the polarized sorting of proteins.

Lipid rafts may be important in the formation of supramolecular protein complexes on the cell surface. These complexes may be important for rapid regulation of receptor activation and the resultant intracellular signaling cascades. The EAATs may be able to form such supramolecular complexes that are dependent on association with lipid rafts. The cell surface expression of EAAT3 is positively regulated by activation of the α isoform of protein kinase C in C6 glioma cells as well as in hippocampal neuron cultures (46, 47). Interestingly, protein kinase Cα is associated with lipid raft microdomains (48). The regulation of EAAT3 surface expression by protein kinase Cα

may depend on their mutual associations with cholesterol-rich, lipid raft microdomains. Identification of those proteins that would interact with lipid raft-associated glutamate transporters would provide novel insights into the supramolecular organization of glutamate transporters and its importance to the function of the EAATs.

In summary, the cell surface expression and plasma membrane distribution of glutamate transporters is regulated by membrane cholesterol. The EAAT family of glutamate transporters is partially associated with novel cholesterol-rich, lipid raft-containing microdomains of the plasma membrane. EAAT2 is more strongly associated with these types of lipid rafts than the other glutamate transporters expressed in the brain. Furthermore, the association of the EAATs with these cholesterol-rich microdomains may be required for glutamate transport activity. This study demonstrates the importance of lipid rafts on the localization and function of Na^+-dependent glutamate transporters in the nervous system.

Acknowledgments—We thank Dr. Jeffrey D. Rothstein for generously providing the EAAT and GTRAP4 antibodies; Dr. Richard W. Burry and the Campus Microscopy Imaging Facility for providing access to the laser scanning confocal microscope; Drs. Georgia A. Bishop and James S. King (Department of Neuroscience) for providing access to their inverted microscope and deconvolution software; and Drs. Karl Obrietan, Arthur H. M. Burghes, and Andrej Rotter for many fruitful suggestions.

REFERENCES

1. Danbolt, N. C. (2001) *Prog. Neurobiol.* **65,** 1–105
2. Rothstein, J. D., Martin, L., Levey, A. I., Dykes-Hoberg, M., Jin, L., Wu, D., Nash, N., and Kuncl, R. W. (1994) *Neuron* **13,** 713–725
3. Conti, F., DeBiasi, S., Minelli, A., Rothstein, J. D., and Melone, M. (1998) *Cereb. Cortex* **8,** 108–116
4. Coco, S., Verderio, C., Trotti, D., Rothstein, J. D., Volterra, A., and Matteoli, M. (1997) *Eur. J. Neurosci.* **9,** 1902–1910
5. Arriza, J. L., Eliasof, S., Kavanaugh, M. P., and Amara, S. G. (1997) *Proc. Natl. Acad. Sci. U. S. A.* **94,** 4155–4160
6. Duan, S., Anderson, C. M., Stein, B. A., and Swanson, R. A. (1999) *J. Neurosci.* **19,** 10193–10200
7. Davis, K. E., Straff, D. J., Weinstein, E. A., Bannerman, P. G., Correale, D. M., Rothstein, J. D., and Robinson, M. B. (1998) *J. Neurosci.* **18,** 2475–2485
8. Sims, K. D., Straff, D. J., and Robinson, M. B. (2000) *J. Biol. Chem.* **275,** 5228–5237
9. Lin, C. G., Orlov, I., Ruggerio, A. M., Dykes-Hoberg, M., Lee, A., Jackson, M., and Rothstein, J. D. (2001) *Nature* **410,** 84–88
10. Butchbach, M. E. R., Lai, L., and Lin, C. G. (2002) *Gene* (*Amst.*) **292,** 81–90
11. Jackson, M., Song, W., Liu, M. Y., Jin, L., Dykes-Hoberg, M., Lin, C. G., Bowers, W. J., Federoff, H. J., Sternweis, R. C., and Rothstein, J. D. (2001) *Nature* **410,** 89–93
12. Simons, K., and Toomre, D. (2000) *Nat. Rev. Mol. Cell. Biol.* **1,** 31–39
13. Brusès, J. L., Chauvet, N., and Rutishauser, U. (2001) *J. Neurosci.* **21,** 504–512
14. Suzuki, T., Ito, J., Takagi, H., Saitoh, F., Nawa, H., and Shimizu, H. (2001) *Mol. Brain Res.* **89,** 20–28
15. Hering, H., Lin, C. C., and Sheng, M. (2003) *J. Neurosci.* **23,** 3262–3271
16. Becher, A., White, J. H., and McIlhinney, R. A. J. (2001) *J. Neurochem.* **79,** 787–795
17. Tansey, M. G., Baloh, R. H., Milbrandt, H., and Johnson, E. M., Jr. (2000) *Neuron* **25,** 611–623
18. Niethammer, P., Delling, M., Sytnyk, V., Dityatev, A., Fukami, K., and Schachner, M. (2002) *J. Cell Biol.* **157,** 521–532
19. Chamberlain, L. H., Burgoyne, R. D., and Gould, G. W. (2001) *Proc. Natl. Acad. Sci. U. S. A.* **98,** 5619–5624
20. Shouffani, A., and Kanner, B. I. (1990) *J. Biol. Chem.* **265,** 6002–6008
21. Butchbach, M. E. R., Guo, H., and Lin, C. G. (2003) *J. Neurochem.* **84,** 891–894
22. Furuta, A., Martin, L. J., Lin, C. G., Dykes-Hoberg, M., and Rothstein, J. D. (1997) *Neuroscience* **81,** 1031–1042
23. Daniels, G. M., and Amara, S. G. (1998) *Methods Enzymol.* **296,** 307–318
24. Li, X., Galli, T., Leu, S., Wade, J. B., Weinman, E. J., Leung, G., Cheong, A., Louvard, D., and Donowitz, M. (2001) *J. Physiol.* **537,** 537–552
25. Arriza, J. L., Fairman, W. A., Wadiche, J. I., Murdoch, G. H., Kavanaugh, M. P., and Amara, S. G. (1994) *J. Neurosci.* **14,** 5559–5569
26. Toews, M. L., Waldo, G. L., Harden, T. K., and Perkins, J. P. (1984) *J. Biol. Chem.* **259,** 11844–11850
27. Daniels, K. K., and Vickroy, T. W. (1998) *Neurochem. Res.* **23,** 103–113
28. Brown, D. A., and Rose, J. K. (1992) *Cell* **68,** 533–544
29. Röper, K., Corbeil, D., and Huttner, W. B. (2000) *Nat. Cell Biol.* **2,** 582–592
30. Bickel, P. E., Scherer, P. E., Schnitzer, J. E., Oh, P., Lisanti, M. P., and Lodish, H. F. (1997) *J. Biol. Chem.* **272,** 13793–13802
31. Schlag, B. D., Vondrasek, J. R., Munir, M., Kalandadze, A., Zelenaia, O. A., Rothstein, J. D., and Robinson, M. B. (1998) *Mol. Pharmacol.* **53,** 355–369
32. Swanson, R. A., Liu, J., Miller, J. W., Rothstein, J. D., Farrell, K., and Stein, B. A. (1997) *J. Neurosci.* **17,** 932–940
33. Hagmann, J., and Fishman, P. H. (1982) *Biochim. Biophys. Acta* **720,** 181–187
34. Simons, K., and Ikonen, E. (1997) *Nature* **387,** 569–572
35. Tsui-Pierchala, B. A., Encinas, M., Milbrandt, J., and Johnson, E. M., Jr. (2002) *Trends Neurosci.* **25,** 412–417
36. Maekawa, S., Iino, S., and Miyata, S. (2003) *Biochim. Biophys. Acta* **1610,** 261–270
37. Chaudhry, F. A., Lehre, K. P., van Lookeren Campagne, M., Ottersen, O. P., Danbolt, N. C., and Storm-Mathisen, J. (1995) *Neuron* **15,** 711–720
38. Poitry-Yamate, C. L., Vutskits, L., and Rauen, T. (2002) *J. Neurochem.* **82,** 987–997
39. Canolle, B., Masmejean, F., Melon, C., Nieoullon, A., Pisano, P., and Lortet, S. (2004) *J. Neurochem.* **88,** 1521–1532
40. Eckert, G. P., Igbavboa, U., Müller, W. E., and Wood, W. G. (2003) *Brain Res.* **962,** 144–150
41. Marchand, S., Devillers-Thiéry, A., Pons, S., Changeux, J. P., and Cartaud, J. (2002) *J. Neurosci.* **22,** 8891–8901
42. Cheng, C., Glover, G., Banker, G., and Amara, S. G. (2002) *J. Neurosci.* **22,** 10643–10652
43. Ledema, M. D., Simons, K., and Dotti, C. G. (1998) *Proc. Natl. Acad. Sci. U. S. A.* **95,** 3966–3971
44. Shayakul, C., Kanai, Y., Lee, W. S., Brown, D., Rothstein, J. D., and Hediger, M. A. (1999) *Am. J. Physiol.* **273,** F1023–F1029
45. Slimane, T. A., Trugnan, G., van Ijzendoorn, S. C. D., and Hoekstra, D. (2003) *Mol. Biol. Cell* **14,** 611–624
46. González, M. I., Kazanietz, M. G., and Robinson, M. B. (2002) *Mol. Pharmacol.* **62,** 901–910
47. González, M. I., Bannerman, P. G., and Robinson, M. B. (2003) *J. Neurosci.* **23,** 5589–5593
48. Mineo, C., Ying, Y. S., Chapline, C., Jaken, S., and Anderson, R. G. W. (1998) *J. Cell Biol.* **141,** 601–610